Malaysian Journal of Computer Science, Vol. 18 No. 1, June 2005, pp. 78-92

SALFSAR: A DUAL PURPOSE DEVICE FOR LAPAROSCOPIC TRAINING AND TELE-SURGERY

Rosli Salleh and Zaidi Razak
Faculty of Computer Science and Information Technology
University Malaya
50603 Kuala Lumpur, Malaysia
email: rosli_salleh@um.edu.my

Darwin Caldwell and Rui Loureiro
School of Acoustics and Electronic Engineering
University of Salford, M5 4WT
United Kingdom

ABSTRACT

This paper presents the design of the Salford Laparoscopic Feedback Simulators and Robot (SalFSAR). It is designed as a dual-purpose device i.e. as a laparoscopic manipulator for virtual reality (VR) simulation and also as a surgical robot. A VR environment has been developed to test the applicability of the device for assisting surgeons in laparoscopic surgery procedures.

Keywords: ***Virtual Simulation, Laparoscopic Training, Surgical Robot, Tele-surgery***

1.0 INTRODUCTION

There is an increasing need to train surgeons in minimally invasive surgery (MIS) since the demand for the procedure is increasing [1]. One method of training is by integrating human-computer interface hardware and VR simulation software, which can mimic the procedure. The human-computer interface hardware may take the form of a laparoscopic tool. There are a few reported works on laparoscopic surgical manipulators for training purposes. The commercial Laparoscopic Surgical Workstation, Laparoscopic Impulse Engine and Virtual Laparoscopic Interface from Immersion Corporation [2] are three good examples. Another example is a PantoScope system that was developed by the Swiss Federal Institute. In the area of surgical robots, there are also several reported works such as DALSA [3], Intuitive [4], ARTEMIS [5] and the "tele-microsurgical" robot [6]. These robots are used to assist surgeons in surgical tasks.

This paper will present a unique approach in our design i.e. a device that can be configured as a laparoscopic training manipulator and as a surgical robot. The device is integrated with a VR environment developed with WorldToolKit. The environment simulates Laparoscopic surgical procedures such as maneuvering the laparoscopic tools, grabbing, touching and cutting tissues.

2.0 DESIGN SPECIFICATIONS

Below are specifications that were taken into consideration when we designed the device:

i) **Similar Design to Real Laparoscope Instruments** - There is an advantage when the mechanical design is similar to the real laparoscopic instruments i.e. the surgeons do not need to familiarise or adapt to the equipment and the 'feel of the real thing' is not changed.

ii) **Position controlled** - One of the limiting factors of the current laparoscope trainers is their rigid design that restricts the control of position of the whole manipulator unit. In real laparoscopic surgeries, at least two ports are created on the patient's body. Each port locates one laparoscopic tool. The ports are first chosen so that they are within the surgical area so that the surgeon can perform the intended task. The surgeon then positions the tools at those ports by inserting the appropriate laparoscopic tools. Therefore, it is an added advantage to be able to control the position of the surgical unit from an out of the way position to the surgical field.

iii) **Simple design and control program** – A simple design will ensure that there is a relatively low number of mechanical parts resulting in easier maintenance, reduced cost and quicker setting up. A simple control program means that stable motion, position and force control loops can be achieved relatively easily. In a

master-slave system, easy translation of control can be achieved if both master manipulators and the slave robots have the same kinematics structure.

iv) **Dual purposes usage** - The tool is to be used as a surgical manipulator and robot. Having a surgical training manipulator and a surgical robot used interchangeably is an added advantage. Both the manipulator and the robot will have a corresponding kinematics structure. Simple changes in configurations and control programs allow the tool to be used as a master or a slave unit.

3.0 CONTROL SYSTEMS

A key part of the use of any manipulator and surgical robot is the control systems that generate the important variables (force, velocity, position etc.), which are vital for the man-machine interface control and are designed to achieve the desired performance criteria for the system. Typical performance criteria include response delay, response time and stability. Fig. 1 (a) shows the basic hardware block diagram of the SalFSAR being used as a manipulator in surgical training. An electronic control unit (ECU) was used for providing the necessary analogue-to-digital and digital-to-analogue conversion. There are two methods in which the manipulator can be controlled, i.e. with and without the strain gauge compensation effect. These can be explained as following:

i) Without the strain gauge, the user provides the necessary force to move the manipulator. Because of the high back-drivability of the motors used, the manipulator can be moved easily. This is exactly the same concept with the Laparoscopic Impulse Engine. In this method, the motors were used to provide 3-DOF force feedback sensation (X, Y and Z-axis force feedback). There are however some frictions in the mechanical parts and also dragging caused by back emf current being generated inside the motors and this does not make the motion in free space as smooth as it would be in a real scenario.

ii) To overcome this dragging/frictional effect, feedforward compensation is used. In this strain gauge effect control, three pairs of strain gauge were used to provide information in tooling control to detect the force applied by the user, which will overcome the friction in the mechanical parts and back emf. The strain gauge reading in this case was transformed into position and became the input to the control system (*set point*) i.e. the position controller. With this method of control, the tool can be driven to and remain in position even though the user has released his hand. This is unlike the first method, where the tool (as well as Laparoscopic Impulse Engine) will return to its rest position if the user releases the tools.

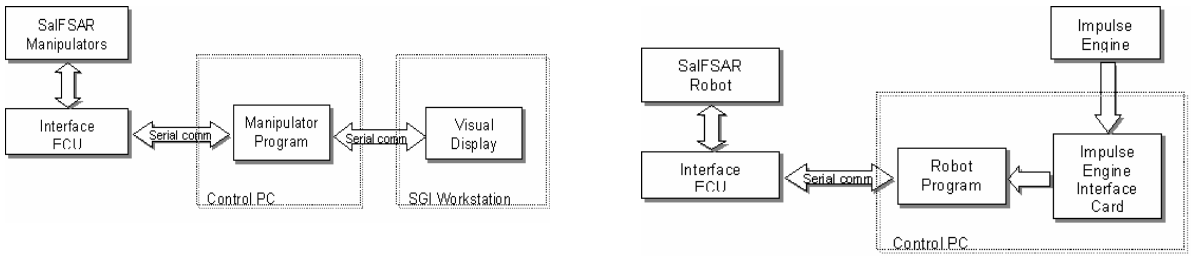

(a) (b)

Fig. 1: (a) SalFSAR as a surgical manipulator. (b) SalFSAR as a surgical robot in a master-slave operation.

Fig. 1 (b) shows the basic hardware configuration of the SalFSAR being used as a surgical robot in a master-slave operation. The "Robot program" was implemented for controlling the slave-manipulator to follow exactly the motion of the master-manipulator. The Laparoscopic Impulse Engine was the master-manipulator and the surgical robot was the slave-manipulator.

4.0 EXPERIMENTS

Several experiments were conducted and are discussed below. The experimental environment showing all the equipment involved is shown in Fig. 2. Fundamentally, one important aspect to be looked at is if the SalFSAR system can cope with the required frequency response i.e. the speed at which the laparoscopic tool is moved. The way this was measured was by making a comparison between the maximum possible speed and frequency of a general laparoscopic operation and the SalFSAR's frequency response.

Experiment results show that the SalFSAR system has:
i) Frequency response which is higher than the existing maximum determined motion frequency
ii) The acceptable step response
iii) Tracking sine-wave input very closely below 1.0 Hz.

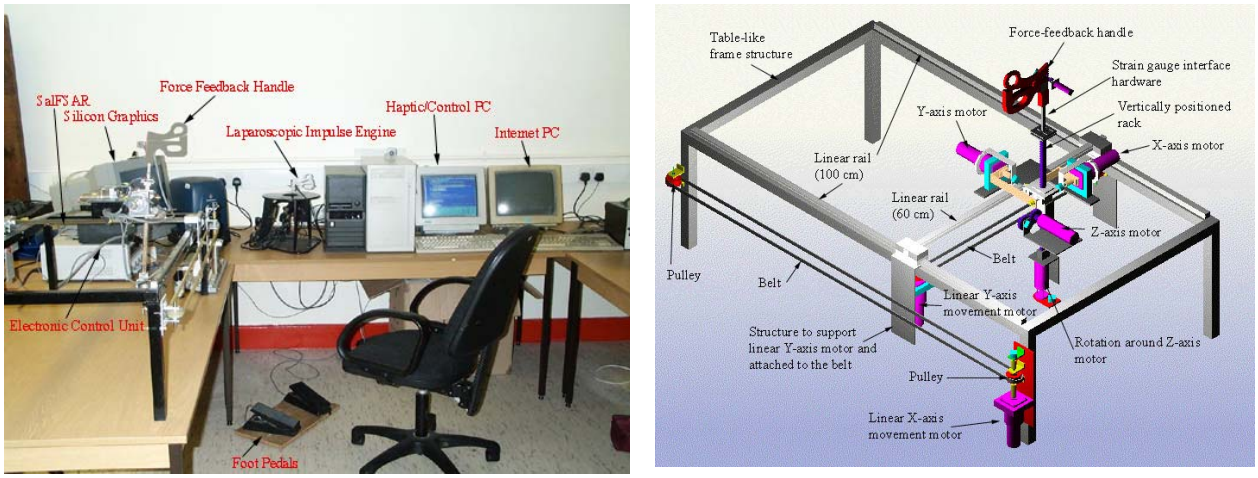

(a) (b)

Fig. 2: (a) Experiment equipment. (b) SalFSAR mechanical structure.

4.1 SalFSAR Motion Ranges and Work Volume

One of the tasks in the experiments is to determine the SalFSAR joint motion ranges and the work volume provided to the operator. A comparison of the motion ranges of the SalFSAR against the Laparoscopic Impulse Engine is presented in Table 1. The first column gives the range of motion of the Laparoscopic Impulse Engine. The second column presents the range of motion of each SalFSAR joint.

From Table 1, it can be seen that the range of motion of the SalFSAR joints is bigger than the corresponding Laparoscopic Impulse Engine motions except for the handle opening, however, the SalFSAR has force feedback where the Impulse engine is only an input device. Bigger motions mean better access to the surgical area. In addition, there are two additional degrees of freedom with the SalFSAR as compared to Laparoscopic Impulse Engine i.e. the linear X and Y-axis translation. The lengths of these links are 100 cm and 60 cm respectively. However, because of the mechanical structure constraints, the actual motions are around 80 cm and 40 cm respectively.

The SalFSAR when used as a surgical manipulator has a partial rotation around the Z-axis. The value was measured as approximately 90 degrees. When it is to be used as a surgical robot, the rotation around the Z-axis motor provides 360 degrees of rotation motion.

Further experiments measure the X, Y and Z-axis motions (detailed in [7]). The results of these measurements are as follows:

X motion ~ -28 cm to +30 cm
Y motion ~ -29 cm to +30 cm
Z motion ~ -21 cm to +5 cm

Table 1: Motion Ranges for the SalFSAR Joint Axis

	Laparoscopic Impulse Engine (degree/cm)	SalFSAR (degree/cm)
X-axis	~ 60 deg	~ 90 deg
Y-axis	~ 60 deg	~ 90 deg
Z-axis	~ 13 cm	~ 26 cm
Rotation around Z-axis	360 deg	~ 90/360 deg
Handle	~ 20 deg	~ 10 deg
Linear X-axis translation	Not existing	~ 80 cm
Linear Y-axis translation.	Not existing	~ 40 cm

In addition to these motion ranges, as discussed earlier the SalFSAR has two additional DOF i.e. the linear and X and Y-axis translation. If the unit is initially placed at the middle, this additional translation motion allows another ±40 cm and ±20 cm for the X and Y-axis respectively. Therefore the whole structures allow the following motion ranges:

X motion ~ -68 cm to +70 cm
Y motion ~ -69 cm to +70 cm
Z motion ~ -21 cm to +5 cm.

4.2 Force Feedback Measurement

Experiments have been conducted on the SalFSAR system to measure the maximum force on the three axes i.e. the X, Y and Z-axis. A dynamometer was attached to the end of the SalFSAR's tooling and the maximum force was read (Fig. 3). From the observations made, as would be expected, the length of the lever contributes to the amount of force that is measured. The shorter the lever from the pivot point, the greater the force. The force measurement results (at 15 volts power supply) for the three axes are:

X and Y-axis = ~ 6 Newton to 12 Newton (when the tooling is fully inserted and extracted respectively)
Z-axis = ~ max of 25 Newton.

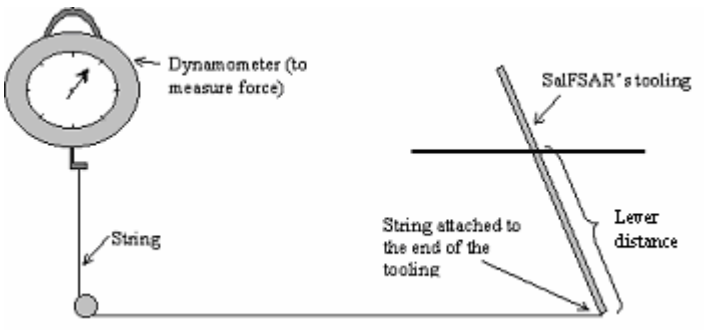

Fig. 3: Measuring forces on SalFSAR's tooling for the X and Y-axis

From the theoretical results [7], the maximum possible force at the tip of the tooling for the X and Y-axis motors are between 6.7 N to 14.6 N. For the Z-axis motor, the maximum possible force is 33 N. The results obtained from the experiment are less than the theoretical results because of possible friction and gravity compensation, which were not taken into account in the theoretical calculation. For the Z-axis motion, the friction and backlash were expected to contribute to the high difference in the result.

4.3 Manipulation and Force Feedback

A program has been created to test the SalFSAR force feedback during manipulation in which the user manipulates the SalFSAR tooling and the movement can be monitored on the computer screen that runs the program. For the program a series of virtual objects have been created consisting of two springs (i.e. horizontal and vertical springs) and a round object (Fig. 4). The horizontal spring is used to test the force feedback on the X-axis and the vertical spring is for testing the Y-axis force feedback.

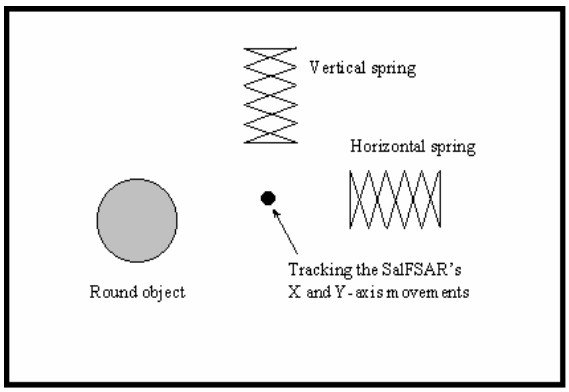

Fig. 4: The testing program created for testing the X and Y-axis force feedback of the SalFSAR

Five different qualitative levels of stiffness have been defined i.e. no stiffness, very soft, soft, hard and very hard (these values were qualitative). The stiffness levels were chosen by varying the proportional constant, K_P, at the following intervals: 0.0, 15.0, 35.0, 55.0 and 75.0 for the no stiffness to very hard levels respectively. Six subjects (all males, aged between 25 to 30 years old) undertaking the experiments were asked to differentiate each of the above levels of stiffness.

To test the combination of the force axes (X and Y-axis) effects, the round object was used. The subjects were instructed to manoeuvre the tool and touch the round object and express their feelings. The stiffness in this case was fixed to very hard so that the user would not be able to penetrate into the round object easily. In another set of tests, the Z-axis force feedback was tested by pushing down and pulling up on the SalFSAR's tooling (the stiffness constants were 0.0, 5.0, 10.0, 20.0 and 30.0).

After the three series of tests for each of the subjects, the results in Fig. 5 were recorded. From the results obtained, a general conclusion was that all the subjects could feel the different levels of stiffness. All the subjects could identify the "no stiffness" level correctly. Almost all subjects (i.e. 99.33%) identified the "very hard" feeling correctly, which was the second best result achieved. 86.67% of the subjects matched the "very soft" feeling correctly, 66.67% of the subjects matched the "soft" feeling correctly, whereas 60.0% of the subjects matched the "hard" feeling correctly. From the result, it shows that the three medium-values of stiffness (very soft, soft and hard) were harder to identify. One reason that can be identified was that there was a bit of confusion between the three during the testing.

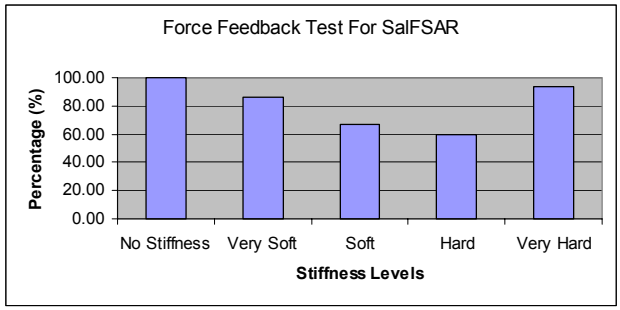

Fig. 5: Force feedback testing for the X and Y-axis of the SalFSAR

All of the subjects could also easily notice the drop of the force when they maneuvered the tool over the edge of the spring. In the identifying round object test, all of the subjects reported the realistic feeling of a round object. Also from observation, all the subjects can be seen maneuvering the tool making a circle around the round object. The results for tracking the round object are shown in Fig. 6. The results show the X and Y-axis motions made by the subjects.

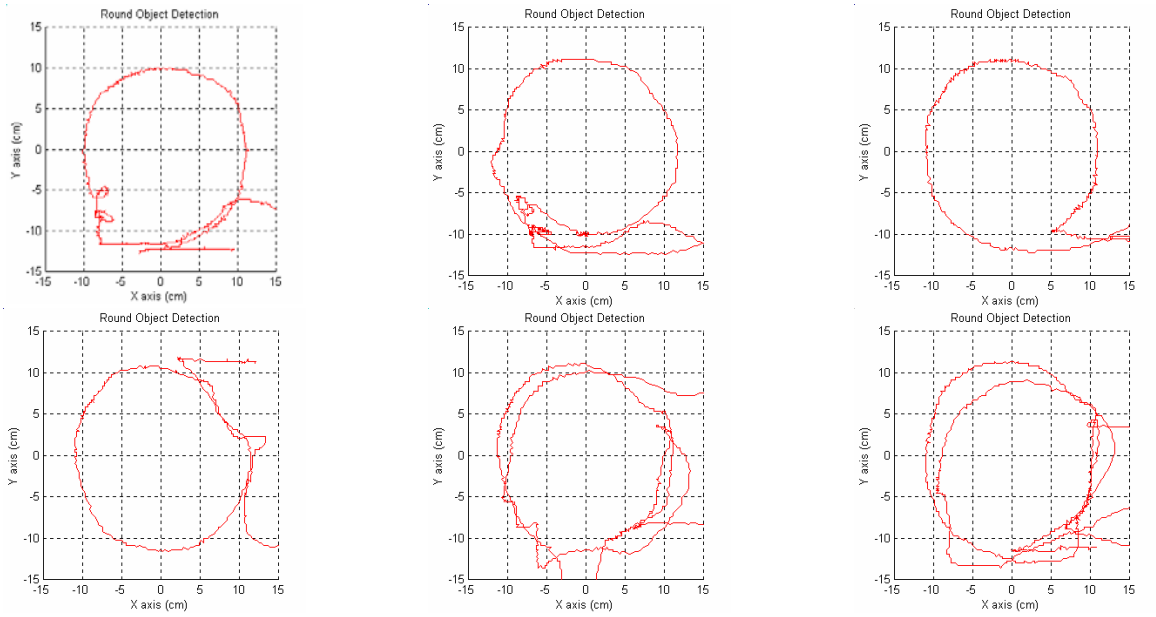

Fig. 6: Results for tracking the round object by the six subjects

In the Z-axis testing, all of the subjects could identify that there were different levels of stiffness. However, to differentiate the levels of stiffness correctly was found to be harder compared to the X and Y-axis experiments. These are due to the frictions on the Z-axis movement and the bad mechanical connection that links the linear and rotary gear (connected to the Z-axis motor). They, however, could easily identify the free movement without any mistakes.

4.4 Manipulation with Strain Gauge Effect

To produce this effect, three pairs of strain gauges (Fig. 7) were used to determine the direction of movement and estimate the voltages to be supplied to the motors so that they would compensate for the drag mentioned above. Using the strain gauges, four combinations of different graphs can be plotted when the user is trying to move the tool to his left, right, forward, and backward (referring to hand motions, which are opposite to tip motions). The results are shown in Fig. 8. The values from these gauges were the input to the control system used to calculate the feedforward response.

From the results obtained, it is possible to identify the four different combinations of sensory effects when the user performs the four movements (backward, forward, right, and left). These graphs are a result of the cross-coupling among the strain-gauge pairs. The effects are seen as discrete actions, not forces or movements related to the measured strains, and have been classified into sections using a technique drawn from fuzzy logic. Three states have been declared i.e. : **No effect** – where the strain gauges reading is between –10 and 10; **Positive** – where the strain gauges reading is greater than 20; **Negative** – where the strain gauges reading is less than –20. These are classified in Table 2.

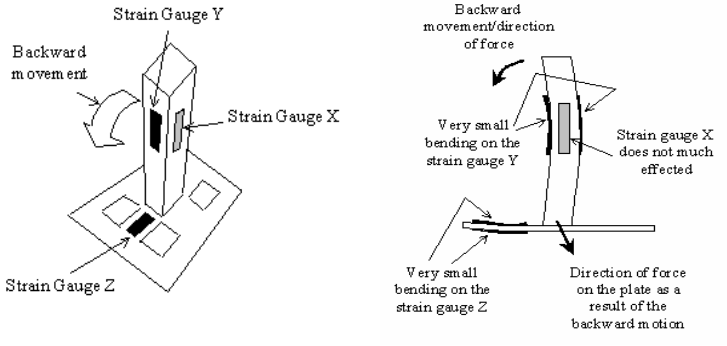

(a) (b)

Fig. 7: The Strain Gauge Interface Hardware- thin block and cross structure plate that housed the three strain gauges pairs. The backward movement causes the strain gauge Y and Z to bend. In reality the bending is too small to be seen by the naked eye. (a) Perspective view of the structure. (b) Front view

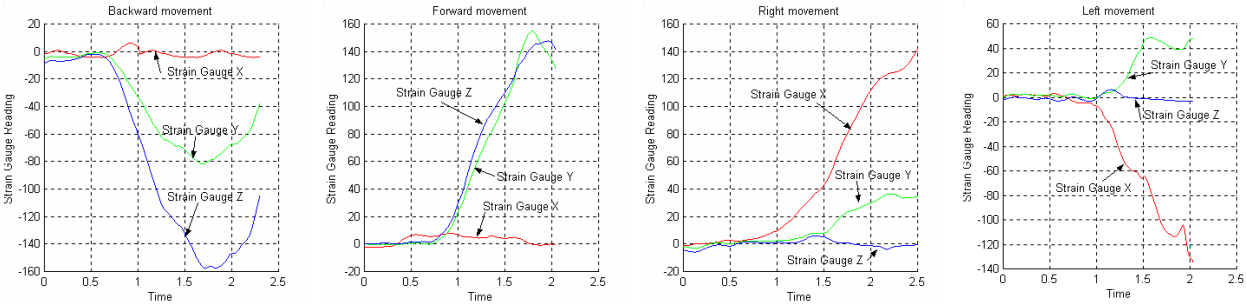

(a) (b) (c) (d)

Fig. 8: Four different combinations of the force measured from the strain gauges for the X, Y, and Z-axis position of the strain gauges. (a) Backward movement. (b) Forward movement. (c) Right movement. (d) Left movement.

Table 2: Unique identities for the backward, forward, right and left movements

Movements	Strain Gauges		
	X	Y	Z
Backward	No effect	Negative	Negative
Forward	No effect	Positive	Positive
Right	Positive	Positive	No effect
Left	Negative	Positive	No effect

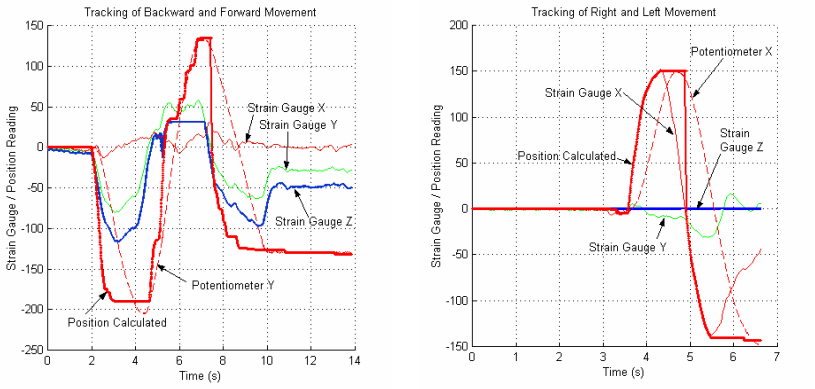

(a) (b)

Fig. 9: Using strain gauges to detect the movements and calculate the position. (a) Backward and forward movement. (b) Right and left movement.

In general, the *Position Calculated* is given as follows:
Position Calculated = *Prev_Pos* + *Rate_of_Change* × *k,* where

$$Rate\_of\_Change = \frac{Current\_strain\_gauge\_reading - Prev\_reading}{dt}$$

The results of the strain gauge readings were captured and analysed with MATLAB and the constant value *k*, was determined.

The results in Fig. 9 (a) and (b) show that the *Positions Calculated* are closely tracking the actual coordinate given by the potentiometers ('*Potentiometer Y*' for the backward and forward movement, and '*Potentiometer X*' for the right and left movement).

Similar testing has been undertaken on the Z-axis. The graph that characterizes and uniquely identifies the Z-axis' downward movement is shown in Fig. 10. A similar calculation was done to measure the *Position Calculated*, with the strain gauge Z used to measure the *Rate_of_Change* (negative value).

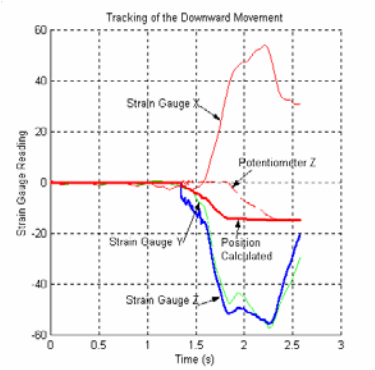

Fig. 10: Strain Gauges reading for the downward Z-axis movement and the position calculated

For the upward movement, the pressure sensor positioned at the bottom of the handle was the switch that indicates that the user is pulling the tooling up. The amount of pressure given was set to be proportional to the voltage supplied to the motor that controlled the upward movement. The results of two different amounts of pressure and the movement induced in the motor (given by the Z-axis potentiometer reading) are given in Fig. 11. As can be seen, the first graph shows a quicker movement compared to the second one. A slightly modified equation was used to measure the *Position Calculated* for the upward movement as follows:

Position Calculated = *Prev_Pos* + (*Pressure_reading* – *Const*) X *k*, where

Const is a dead-band constant value chosen so that if the reading of the pressure sensor is below this value, there is no change in the *Position Calculated* and *k* is the proportional constant which was determined after analysis with the MATLAB software.

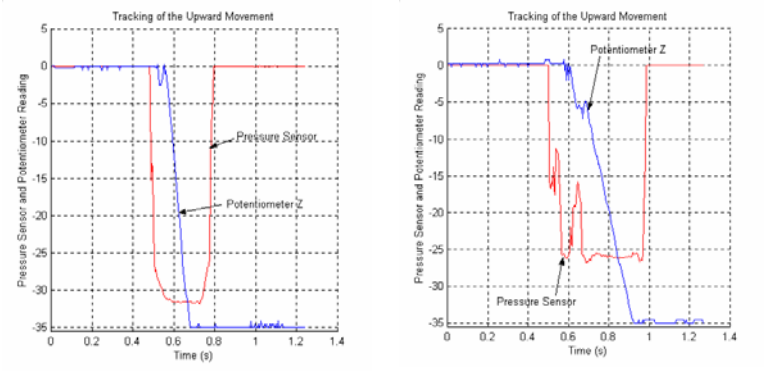

(a) (b)

Fig. 11: Results of two different rate of change for the pressure sensor and the potentiometer position. In (a) the user presses the sensor stronger than in (b).

The summary for the valid ranges and the constant, *k* values for all of the movements discussed above is given in Table 3.

Table 3: Defining the rate of change, valid range and the constant k

Movement	Rate of Change	Valid Ranges	K
Backward	-From Strain Gauge Y -Negative value	Strain Gauge Y – Negative, Strain Gauge X – No Effect, and Strain Gauge Z – Negative	2.955
Forward	-From Strain Gauge Y -Positive value	Strain Gauge Y – Positive, Strain Gauge X – No Effect, and Strain Gauge Z – Positive	4.555
Left	-From Strain Gauge X -Negative value	Strain Gauge X – Negative, Strain Gauge Y – Positive, and Strain Gauge Z – No Effect	1.055
Right	-From Strain Gauge X -Positive value	Strain Gauge X – Positive, Strain Gauge Y – Positive, and Strain Gauge Z – No Effect	1.055
Downward	-From Strain Gauge Z -Negative value	Strain Gauge Z – Negative, Strain Gauge X – Positive, and Strain Gauge Y – Negative	3.255
Upward	-From Pressure Sensor	Pressure Sensor >= 20.0	0.085

From the results shown, we have managed to use the three pairs of the strain gauge to control the five motions of the tool by measuring the strain gauge values and identifying the type of motions. However the system was not calibrated to detect motion in any direction. This was because of its inability to identify unique identities for any-direction motion. For example, it was found that the 45^{o} forward-right motion has a similar graph to the forward motion. Furthermore, any direction can also be 46^{o} forward-right, which obviously has very similar (if not exactly the same) motion as the 45^{o} motion. This limitation however does not mean that the SalFSAR has limitation in its motion. The ability to control the four directions of motions (backward, forward, right and left) allows any direction of motion by combining each of the motions.

4.5 Force Feedback Handle and Cutting Simulation

The Laparoscopic Impulse Engine instrumentation does not have an active feedback to the handle and this means that it was not possible to emulate grasping and cutting of tissues. As previously described, however, there is a force feedback handle in the bespoke force reflection system. Testing of the handle grip feedback mechanism revealed that it could generate a maximum force of approximately 6N with an angle of travel of 10^{o}.

To test the ability to clamp and cut through tissues and the quality of the experience, a simple experiment was conducted whereby a virtual image of a vein/artery/tendon was constructed together with an MIS tool with an appropriate end section (Fig. 12). Within the virtual environment, the tool can be manipulated to grasp tissues or to dissect them. During the clamping or cutting operations, the forces on the scissors were measured and recorded.

The first step in the testing is to define a control method for simulating the stiffness and viscosity sensation during clamping/grasping. The proportional and derivative (PD) control method has been employed where varying the proportional constant, *Kp*, controls the stiffness sensation, and varying the derivative constant, *Kd*, controls the viscosity sensation.

In the initial test, an arbitrary trial and error for the selection of the two constants (*Kp* and *Kd*) was made, while in the actual test, third parties were involved. Two types of results are presented here i.e. grabbing/clamping (Fig. 13 (a)) and cutting (Fig. 13 (b)), while varying the *Kp* and *Kd*.

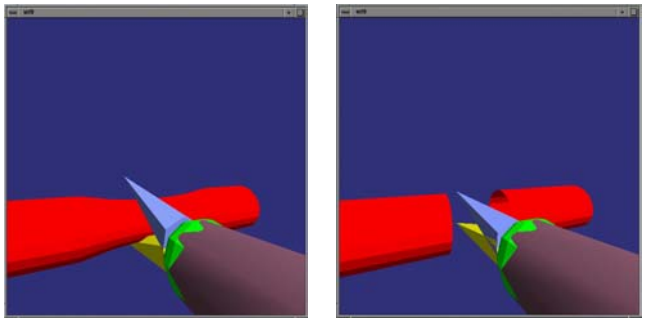

(a) (b)

Fig. 12: Simulation of a virtual vein being cut. (a) Before the cutting operation. (b) After the cutting operation.

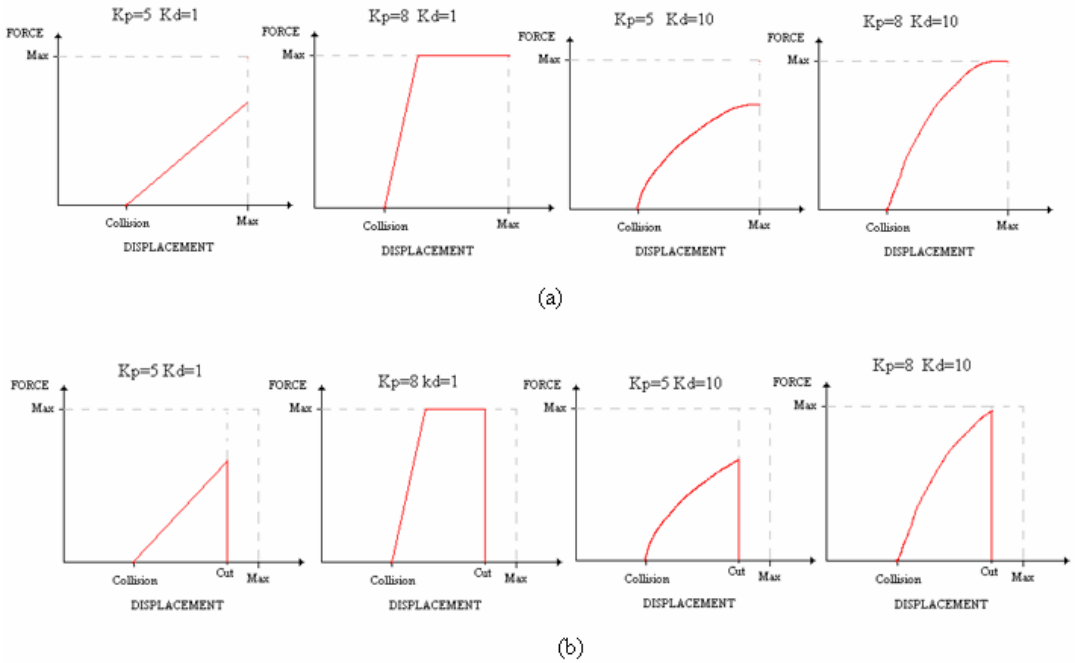

Fig. 13: Responses with different levels of stiffness and viscosity, (a) grabbing, (b) cutting

The test has gone further to include the feedback from the third party users. Six test subjects (none of whom have medical experience) were asked to perform a series of grasping and cutting operations. All subjects could feel when a collision with the vein occurred, when cutting happened and could distinguish the different levels of force. In the grabbing procedure, 66.6% of the subjects could feel the difference between the different levels of stiffness and viscosity. They reported the response for Kp=5 and Kd=1 as being a stiff sensation and Kp=8 and Kd=1 as being highly stiff, increasing linearly until they reach their maximum displacement. For Kd=10 (high viscosity), an exponential increase in the force was reported. The subjects have described this force as being a sort of viscose sensation more associated with a less stiff force but having the same magnitude as with the simulation using Kd=1 (stiff). Although the subjects could feel the difference between the different levels of stiffness, 33.4% reported that they could feel only two levels of force; a small magnitude continuous force applied from the start until the point of collision and the grabbing force.

In the cutting procedure, 50% reported the feeling of cutting through a material with some level of elasticity. 25% reported that they could feel the cutting point only for *Kp*=5 and *Kd*=10 (highly viscosity). The remaining 25% of the subjects were unable to differentiate the cutting sensations.

4.6 Tele-Surgical Robot

One of the most important tests is the control of the robot (SalFSAR). The test on the surgical robot was performed using the Laparoscopic Impulse Engine acting as a master and the Salford Surgical Robot unit as a slave. The *Robot control software* was implemented to read the Impulse Engine positions and control the robot to follow the positions

exactly. The proportional, integral and derivative (PID) controller was implemented to position and orient the end effector with a specific speed and precision. The results in Fig. 14 show that the robot is tracking the slave with a minimal phase difference (less than 5 degrees) giving a desired performance.

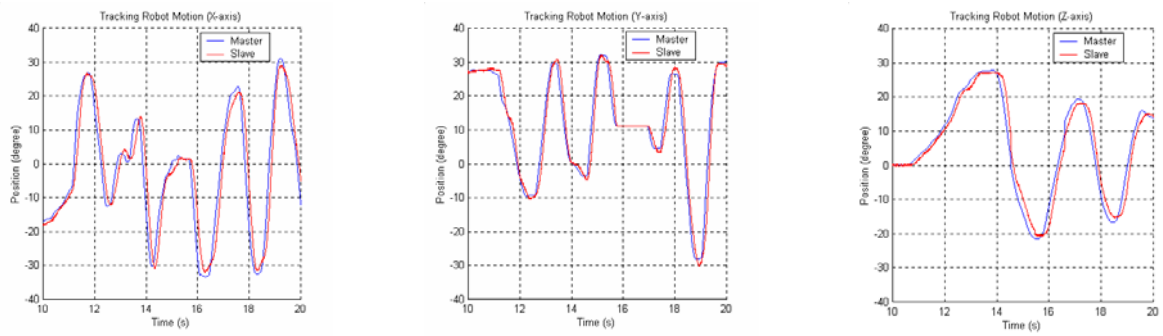

(a) (b) (c)

Fig. 14: Robot Master-Slave operation using PC30A for the (a) X-axis, (b) Y-axis, and (c) Z-axis

4.7 VR Experiment

The VR system that was being developed ultimately has the goal of being used in training medical students to perform laparoscopic surgery procedures such as maneuvering the tool, grasping tissue, cutting a vein, and studying the problems faced by the users/training 'surgeons'. For this paper, several VR environments were developed to study some aspects of these procedures. The outline of the experiments is as follows:

4.7.1 Grabbing Simulation

In a real laparoscopic surgery, a surgeon will manipulate tools inside a patient's body and perform an intended task. This task always requires the surgeon to grab part of the organ such as in a cutting procedure. In this procedure, the surgeon has to grab part of the organ before performing the cutting.

A simple technique that manipulates the vertices of the polygons has been employed. The vertex of a virtual skin where the virtual scissor touches becomes the centre stretching point. When the user stretches the skin, the centre vertex will follow the position of the tip of the virtual scissors. The surrounding vertices will also set to move toward the stretching point but with lesser displacement. The result of the experiment is shown in Fig. 15 when the user grabs the tissue of the stomach.

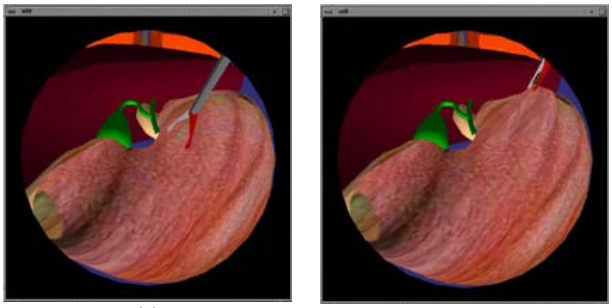

(a) (b)

Fig. 15: Grabbing the tissue of the stomach. (a) Before grabbing. (b) During grabbing.

The haptic test undertaken with this simulation involved exploration of the virtual environment, touching, grasping and stretching objects. During the test, the user was able to feel the stretching forces. These forces were reported to be real or perhaps realistic. Even though the system managed to detect the contact between the virtual surgical tool and the organs, many improvements still need to be made to provide a true feeling of force to the user.

4.7.2 Cutting Simulation

In many surgical procedures, the cutting of tissues is involved or is part of the procedure, for example in gallbladder removal. A simple technique of cutting has been simulated on a model of a vein/ligament/cartilage. This technique

involves the deformation of the vein before it is cut (Fig. 16). The hardware that was used to simulate this behaviour is the force feedback handle, which is part of the SalFSAR system.

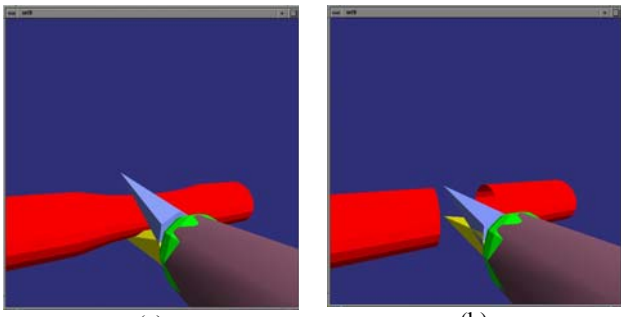

(a) (b)

Fig. 16: Simulation of a virtual vein being cut. (a) Before cutting operation. (b) After the cutting operation.

4.7.3 3D Depth View Problem

One of the problems in a VR simulation is the inability to display the correct view of depth perception in the virtual environment [8]. Also, in a real MIS surgery, one of the problems is that the surgeon has to adjust to a two dimensional view rather than three dimensional. In both cases, lack of depth perception may cause the user to be unable to locate and maneuver the surgical tool accurately. This will affect his or her performance and may cause damage to the surrounding tissues.

The focus of this section is on VR training with the aim of solving the depth perception problem using a very simple method. Using an augmented reality technique, this concept can be applied to real MIS surgeries. An index is introduced to the simulation (Fig. 17). The experiment requires each subject to maneuver the virtual laparoscopic tool using the Laparoscopic Impulse Engine and to touch the markers (represented as a dark coloured triangle) on the simulated skin of the stomach. Five different marks will be revealed one after another and the sequence of these marks can be changed between experiments. Two measurements were recorded i.e. *Completion time* – time taken to finish all the tasks, and *Percent of errors* – percent of touching the wrong spot.

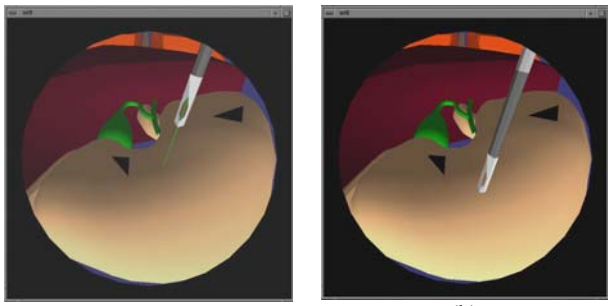

(a) (b)

Fig. 17: Snapshot of an endoscopic view of a virtual laparoscopic environment designed for testing. The environment consists of a virtual laparoscopic tool and several organs (stomach, gallbladder, liver and lungs). Two different experiments were conducted. (a) Laparoscopic tool with an index. The index is a green tiny cylinder as an extension to the laparoscopic tool. (b) Laparoscopic tool without an index.

Eight subjects (all males, aged between 20 to 26 years old), who have no previous experience whatsoever with the laparoscopic tool manipulation, were involved in these experiments. Two sets of experiments were conducted on each subject. In the first experiment, the 'index' was attached to the tool and in the second experiment the index was removed. The second experiment was conducted as soon as the first experiment had been completed. Results of the experiments are shown in Fig. 18 (a) and (b).

From both experiments, several important conclusions can be made:

i) In both instances there is a learning effect with both methods showing progress in terms of the number of errors made and the time taken to complete a given task

ii) With the index, it greatly helps the users to maneuver the tool as can be seen from the results. Generally, even though the users have shown good progress towards the end of the indexed experiment, when asked to perform the experiment without the index, their performance degraded. This was understood to be caused by the 3D depth perception problem.

iii) The VR training system developed is especially good for error improvement (particularly in tool maneuvering) in which the users can practice as many times as they like to try and minimize the errors.

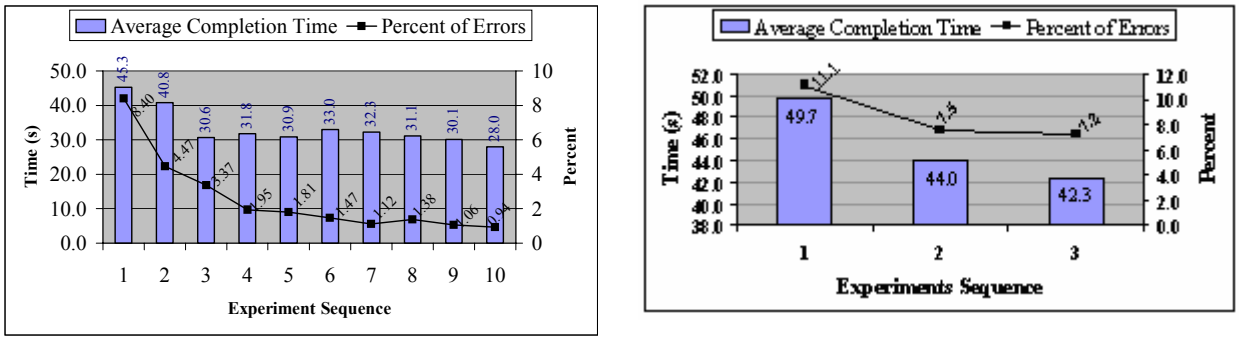

(a) (b)

Fig 18: (a) Experiment result with index. (b) Experiment result without index.

4.7.4 Force Feedback During Manipulation

Force feedback is one of the elements that affect the realism of a virtual environment for medical applications. In the VR experiments that have been presented so far, this element has not been integrated into the system. This section will present experiments that combine force sensation in the VR environment. The objective of this section is to make a comparison in terms of the depth of penetration between no force feedback and with force feedback made during operation. In addition, a study will be made in terms of the contribution of the force feedback towards the completion time and maneuvering of the tool. Five subjects (all males, age between 20 to 30 years old), performed two types of experiments – the first one was without force and the second was with force feedback. One of the subjects has a lot of experience in VR tool manipulation. The experiment procedure with the index, as explained in section 4.7.3, was used for both types of experiments. Each experiment was repeated three times and selected at random between the force and no force feedback. The subjects were requested to maneuver the tool and touch the five different spots on the objects. The penetration depth was calculated and captured during the testing.

The results of the first experiments (without force feedback) are shown in Fig. 19. Comparisons between two subjects are shown i.e. the one without much experience in tool manipulation in VR training and the other with a lot of experience. The former subject made about ten counts of touching, with the depth of penetration of up to 11mm. The latter subject made only five counts of touching (the minimum required) with the depth of penetration of up to 5mm and a better completion time. The results show that the experienced user was able to control the tool more competently.

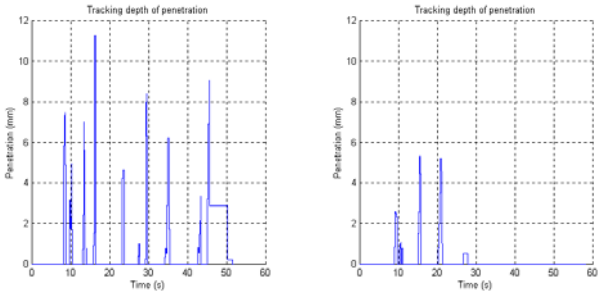

(a) (b)

Fig. 19: Experiment results showing the number of touch made, depth of penetration and completion time for the experiment with no force feedback. Comparison of two typical results was made. (a) A user without much experience. (b) A user that has a lot of experience in manipulating laparoscopic tool in VR training.

The results of the second experiment (with force feedback) are shown in Fig. 20. The performance of the same two subjects as in the previous experiments is plotted. The important observation that is to be made here is in the penetration depth made to complete the tasks for the two subjects. Both subjects made good improvements when there was force feedback on the tool. With force feedback, the inexperienced user made only up to 5.5mm of penetration depth to complete the tasks (as compared to 11mm without force feedback). For the experienced user, the penetration depth was only up to 3.5mm (as compared to 5mm without force feedback). The results for the rest of the subjects are shown in Fig. 21 and Fig. 22, for the no force feedback and with force feedback respectively.

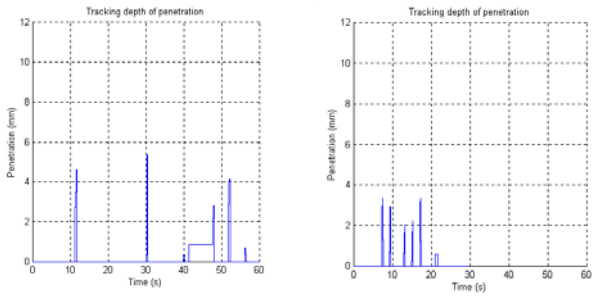

(a) (b)

Fig. 20: The experiment with force feedback. Again comparison was made to show the performance of the same two users. (a) A user without much experience. (b) A user with a lot of experience in manipulating laparoscopic tool in VR training.

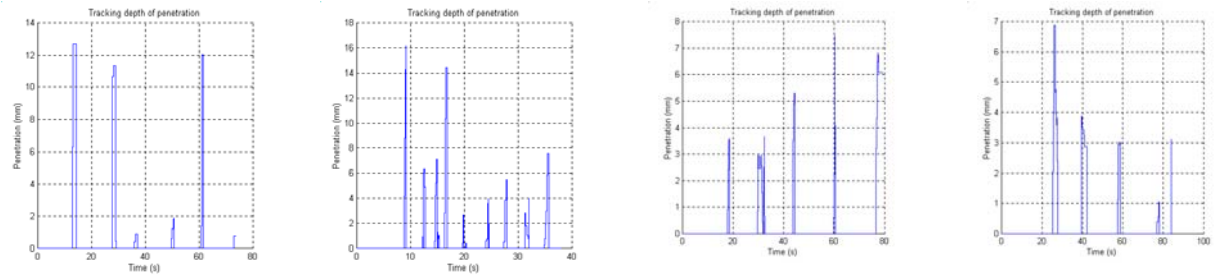

Fig. 21: Experiments without force feedback for the rest of the subjects

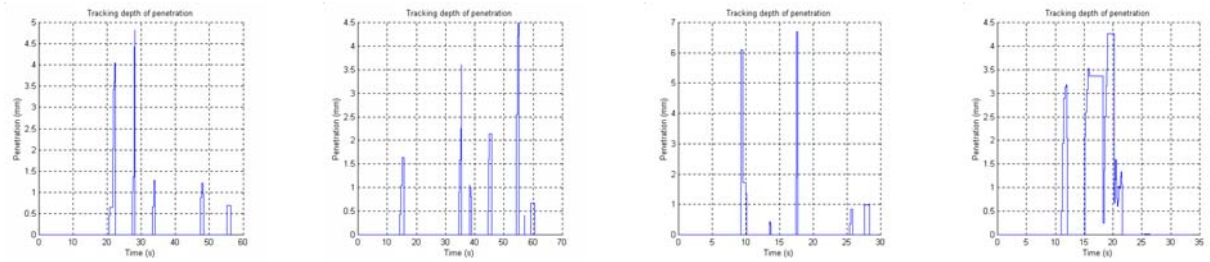

Fig. 22: Experiments with force feedback for the rest of the subjects

With these kinds of experiments, there is no immediate proof to say that the force feedback feeling helped the users to complete the task faster. This can be seen from the completion time made by the two subjects i.e. around 51 sec (without force feedback) and 67 sec (with force feedback) for the inexperienced user. For the experienced user, the completion time was around 28 sec (without force feedback) and 21 sec (with force feedback). There is also no proof to say that there was any improvement in terms of the total counts of touching made (out of supposedly five touching). The first subject showed good improvement i.e. from 10 touching to 6 touching but the second subject's performance had declined i.e. from 5 touching to 6 touching.

5.0 CONCLUSIONS

This paper introduces SalFSAR which is a dual-purpose device, with a 7 degree-of-freedom (DOF) laparoscopic manipulator and a 6 DOF surgical robot. In the laparoscopic manipulator configuration, it has 4 DOF providing

force feedback i.e. the X, Y and Z-axes and an additional one DOF from the force feedback handle. There are several specifications of the SalFSAR that stress the advantages and uniqueness of its design. One important aspect is its dual-purpose usage. Additional control using strain gauges allows it to be driven freely (reducing friction). It can also be positioned on a workspace and the tool will stay on its position even though the user releases his hand from it. Additional X and Y-axis linear movements allow for a bigger workspace for the overall system. This aspect allows us to position the surgical unit from an out of the way position into the surgical field. Another very important aspect that has been looked at is the sensation of force feedback on the user's hand. This sensation has been effectively integrated into the simulation system. The work on force feedback handle provides additional feedback on the fingers of the user. The experiments conducted show the effectiveness of the VR system developed in identifying certain problems (e.g. 3D depth perception and force feedback during manipulation) and in training new surgeons. A simple method i.e. by adding an 'index' has helped to reduce the 3D depth perception problem. Using an augmented reality technique, these methods can be applied to real surgical scenarios.

6.0 REFERENCES

[1] A. Rovetta and R. Sala, Telerobotic Surgery Project for Laparoscopy. *Robotica,* Vol. 13, July/August 1995, pp. 397-400.

[2] Immersion Corporation, http://www.immersion.com/medical/products/laparoscopy/hardware.php>. (Access 20th July 2003).

[3] M. Minor and R. Mukherjee, A Dexterous Manipulator for Minimally Invasive Surgery. *Proceedings of the 2000 IEEE International Conference on Robotics & Animation*, May 1999, pp. 2057-2064.

[4] G. S. Guthart, and J. K. Salisbury, The Intuitive Telesurgery System: Overview and Application. *Proceedings of the 2000 IEEE International Conference on Robotics & Animation*, April 2000, pp. 618-621.

[5] Forschungszentrum Karlsruhe. *ARTEMIS Homepage.* <http://wwwserv2.iai.fzk.de/~artemis/welcome_engl.html>. (Access 20th July 2003).

[6] M. Mitsuishi, et al. Remote Operation of A Micro-surgical System. *Proceedings of the 1988 IEEE, International Conference on Robotics & Automation,* May 1998, pp. 1013-1019.

[7] R. Salleh, "Minimally Invasive Surgery Training and Tele-Surgery System Using VR and Haptic Techniques", *PhD Thesis*, Telford Research Institute, School of Acoustics and Electronic Engineering, University of Salford, UK, April 2001.

[8] P. Rokita, "Generating Depth-of-Field Effects in Virtual Reality Applications". *IEEE Computer Graphics and Applications*, Vol. 16 (No.2), Mar 1996, pp.18-21.

BIOGRAPHY

Rosli Salleh received his PhD in 2001 from the University of Salford, UK. He is currently a lecturer at the Faculty of Computer Science and Information Technology, University of Malaya.

Zaidi Razak is a lecturer at the Faculty of Computer Science and Information Technology, University of Malaya. His main research area is in image processing and he is currently doing research for his PhD.

Darwin Caldwell is a Professor at the School of Acoustics and Electronic Engineering, University of Salford, UK. His main research interest is in robotic.

Rui Loureiro was a Master Student at the University of Salford in the year 2000. He greatly contributed towards the design of the force feedback handle.